UCSF
UC San Francisco Previously Published Works

Title

Long-term, dynamic synaptic reorganization after GABAergic precursor cell transplantation into adult mouse spinal cord.

Permalink

https://escholarship.org/uc/item/819272w0

Journal

The Journal of Comparative Neurology, 526(3)

Authors

Llewellyn-Smith, Ida
Bráz, João
Basbaum, Allan

Publication Date

2018-02-15

DOI

10.1002/cne.24346

Peer reviewed

eScholarship.org Powered by the California Digital Library
University of California

Author Manuscript

Author Manuscript

Author Manuscript

Author Manuscript

HHS Public Access

Author manuscript

J Comp Neurol. Author manuscript; available in PMC 2018 November 29.

Published in final edited form as:

J Comp Neurol. 2018 February 15; 526(3): 480–495. doi:10.1002/cne.24346.

Long-term, dynamic synaptic reorganization after GABAergic precursor cell transplantation into adult mouse spinal cord

Ida J. Llewellyn-Smith[1,2], **Allan I. Basbaum**[2], and **João M. Bráz**[2]

[1]Cardiovascular Medicine, Human Physiology and Centre for Neuroscience, College of Medicine and Public Health, Flinders University, Bedford Park, South Australia, Australia

[2]Department of Anatomy, University of California San Francisco, San Francisco, California

Abstract

Transplanting embryonic precursors of GABAergic neurons from the medial ganglionic eminence (MGE) into adult mouse spinal cord ameliorates mechanical and thermal hypersensitivity in peripheral nerve injury models of neuropathic pain. Although Fos and transneuronal tracing studies strongly suggest that integration of MGE-derived neurons into host spinal cord circuits underlies recovery of function, the extent to which there is synaptic integration of the transplanted cells has not been established. Here, we used electron microscopic immunocytochemistry to assess directly integration of GFP-expressing MGE-derived neuronal precursors into dorsal horn circuitry in intact, adult mice with short- (5–6 weeks) or long-term (4–6 months) transplants. We detected GFP with pre-embedding avidin-biotin-peroxidase and GABA with post-embedding immunogold labeling. At short and long times post-transplant, we found host-derived synapses on GFP-immunoreactive MGE cells bodies and dendrites. The proportion of dendrites with synaptic input increased from 50% to 80% by 6 months. In all mice, MGE-derived terminals formed synapses with GFP-negative (host) cell bodies and dendrites and, unexpectedly, with some GFP-positive (i.e., MGE-derived) dendrites, possibly reflecting autoapses or cross talk among transplanted neurons. We also observed axoaxonic appositions between MGE and host terminals. Immunogold labeling for GABA confirmed that the transplanted cells were GABAergic and that some transplanted cells received an inhibitory GABAergic input. We conclude that transplanted MGE neurons retain their GABAergic phenotype and integrate dynamically into host-transplant synaptic circuits. Taken together with our previous electrophysiological analyses, we conclude that MGE cells are not GABA pumps, but alleviate pain and itch through synaptic release of GABA.

Keywords

GABA; spinal cord; structural plasticity; transplants; ultrastructure; RRID:SCR_003970; RRID:SCR_007418; RRID:AB_476667; RRID:SCR_003577; RRID:SCR_008487

Correspondence: João Bráz, Department Anatomy, University California San Francisco, 1550 4th Street, Room 345, San Francisco, CA 94158. joao.braz2@ucsf.edu.

CONFLICT OF INTEREST

The authors have no conflicts of interest to declare.

Author Manuscript Author Manuscript Author Manuscript Author Manuscript

1 | INTRODUCTION

Neuropathic pain is a debilitating chronic condition that results from injury to either peripheral or central neurons. Its hallmarks are ongoing, often burning, pain as well as mechanical and thermal hypersensitivity. Although many factors contribute to the neuropathic pain state, particular attention has focused on loss of dorsal horn GABAergic inhibitory control following peripheral nerve injury. Deficits in dorsal horn inhibition include decreased expression of glutamic acid decarboxylase (GAD), the GABA-synthesizing enzyme (J. M. Braz et al., 2012; Moore et al., 2002), altered chloride gradients that reduce GABA-mediated hyperpolarization (Coull et al., 2005) and changes in pre- and postsynaptic GABA receptors (Fukuoka et al., 1998). Predictably, traditional pharmacotherapy for neuropathic pain involves anti-convulsant drugs that enhance inhibition and reduce hyperexcitability. Unfortunately, adverse side effects from systemic drug administration limit the efficacy of these treatments.

We recently reported that an approach directed at the underlying etiology of neuropathic pain could have beneficial effects and potentially be disease-modifying (J. Braz, Solorzano, Wang, & Basbaum, 2014; J. M. Braz et al., 2012; J. M. Braz, Wang, Guan, Rubenstein, & Basbaum, 2015). We demonstrated that intraspinal transplantation of embryonic precursors of cortical GABAergic interneurons derived from the medial ganglionic eminence (MGE) reversed mechanical allodynia and heat hyperalgesia in two mouse models of neuropathic pain. Based on Fos expression in transplanted neurons induced by noxious stimuli, we suggested that the functional improvement resulted from integration of the transplanted cells into host dorsal horn circuitry. Consistent with this conclusion, we recently demonstrated that optogenetic stimulation of sensory neurons activates transplanted neurons and that optogenetic stimulation of the transplants results in $GABA_A$ receptor-mediated inhibition of host neurons (Etlin et al., 2016). Finally, we studied mice in which the gene that encodes the vesicular GABA transporter had been deleted. In these mice, the transplanted cells survive but are ineffective, confirming that transplant-derived GABA is essential for the anti-hyperalgesic effects of the MGE cells (J. M. Braz et al., 2015). Based on these findings, we concluded that the beneficial effects of the transplants reflected the establishment of new inhibitory dorsal horn circuits in the host. This conclusion differs significantly from the hypothesis that transplants ameliorate neuropathic pain because they act as cell-based GABAergic pumps.

To establish unequivocally that transplanted neurons integrate into host circuitry requires demonstration of synaptic interactions between transplanted MGE-derived neurons and the host. In the present study, we used electron microscopic immunocytochemistry to address this question directly. We show that GFP-immunoreactive MGE cells transplanted into the dorsal horn of naive adult mice form synapses with host (GFP-negative) neurons and that synaptic integration increases substantially between 6 weeks and 6 months after transplantation. GABA immunogold labeling confirmed that the GFP-expressing MGE cells are GABAergic, are under host inhibitory control and, unexpectedly, communicate with each other. From these observations, we conclude (1) that MGE cells undergo synaptic integration into host spinal cord circuitry, even in the absence of nerve injury, and (2) that circuits formed between the host and the transplant are dynamic and evolve over time. Our findings

Author Manuscript Author Manuscript Author Manuscript Author Manuscript

demonstrate a remarkable synaptic plasticity in the normal, uninjured adult spinal cord and establish the anatomical basis for the anti-hyperalgesic effects produced by GABAergic progenitor cell transplants.

2 | METHODS

The Institutional Care and Animal Use Committee at the University of California San Francisco reviewed and approved all experiments.

2.1 | Transplantation of cells isolated from the medial ganglionic eminence (MGE)

MGE cells were harvested at embryonic day 12.5–13.5 from GAD-GFP transgenic mice in which GFP expression is driven by the GAD67 promoter (Gad1tm1.1Tama; J. M. Braz et al., 2012; Tamamaki et al., 2003). Transplants were performed as previously described (J. M. Braz et al., 2012) in naïve 6–8 week-old male or female mice of the same genetic background as the MGE donors (CD1xC57BL6/J). After anesthetizing the recipient mouse with intraperitoneal ketamine (60 mg/kg)/xylazine (8 mg/kg), we exposed a 1.5–2 mm length of the lumbar enlargement through a dorsal hemilaminectomy and incised and reflected the dura mater. We used a glass micropipette and a microinjection apparatus to make four injections of the MGE cell suspension into the dorsal horn of naive mice, each of which received a total of 5×10^4 MGE cells. After wound closure and recovery from the anesthetic, the mouse was returned to its home cage. Mice with transplants were perfused at short (5–6 weeks; $n = 6$), or long (19 or 26 weeks; $n = 3$) times after the transplantation surgery. Motor function was not impaired in any of the mice.

2.2 | Tissue processing

Six mice with short-term MGE transplants (5–6 weeks) and six mice with long-term MGE transplants (5–6 months) were deeply anesthetized with 2.5% avertin and perfused transcardially with 10 ml of DMEM/F12 tissue culture medium (Catalogue #D-8900; Sigma-Aldrich, St Louis, MO) followed by 30 ml of 4% formaldehyde, 0.3% glutaraldehyde in 0.1 M sodium phosphate buffer, pH 7.4. We removed perfused spinal cords and prepared approximately 4 mm long blocks that were centered on the transplant site. Spinal segments containing the MGE transplant were post-fixed overnight at 4°C. Segments from 1 to 3 mice were embedded together in albumin-gelatin (Llewellyn-Smith et al., 2007), which was hardened in phosphate-buffered 4% formaldehyde for 30 min at room temperature and then sectioned transversely at 50 μm on a Vibratome. Two adult GAD-GFP transgenic mice were perfused and processed as for the mice with MGE transplants. We cut 50 μm transverse or sagittal Vibratome sections of the albumin-gelatin embedded cords from the GAD–GFP transgenic mice and 50 μm transverse Vibratome sections of their brains.

2.3 | Pre-embedding immunocytochemistry to localize GFP

To prepare sections for ultrastructural analysis, we used our standard electron microscopic immunocytochemical protocol, which ensures that immunoreagents penetrate completely through a 50 μm thick Vibratome section (Llewellyn-Smith & Minson, 1992). Briefly, the sections were first washed for 2 hr in 50% ethanol in distilled water to improve antibody penetration and then incubated in 10% normal horse serum (NHS; Invitrogen) diluted with

Author Manuscript Author Manuscript Author Manuscript Author Manuscript

10 mM Tris, 0.9% NaCl, 0.05% thimerosal in 10 mM phosphate buffer, pH 7.4 (TPBS), for 30 min to block nonspecific antibody binding. Sections were then incubated in a 1:10,000 or 1:20,000 dilution of chicken anti-GFP antiserum (Abcam, Cambridge, MA; Table 1) in 10% NHS-TPBS, in biotinylated donkey anti-chicken immunoglobulin Y (Catalogue #703-065-155; Jackson ImmunoResearch, West Grove PA) diluted 1:500 with 1% NHS-TPBS and finally in ExtrAvidin-horseradish peroxidase (Catalogue # E-2886; Sigma) diluted 1:1,500 with TPBS. All steps were performed at room temperature on a shaker and incubations in each immunoreagent lasted for 3–6 days. We localized GFP-immunoreactivity in transplanted MGE cells with a nickel-intensified diaminobenzidine (DAB) reaction and glucose oxidase-generated hydrogen peroxide (Llewellyn-Smith, Dicarlo, Collins, & Keast, 2005). We have previously shown that this antibody does not stain sections of perfused central nervous tissue in which GFP is absent (Llewellyn-Smith, Reimann, Gribble, & Trapp, 2011). We used the same protocol to localize GFP-immunoreactivity in sections of brain and albumin-gelatin embedded spinal cord from the GAD-GFP transgenic mice.

Sections from mice with MGE transplants were processed into resin for ultrastructural examination. After washing for 3 × 10 min in 0.1M phosphate buffer, pH 7.4, sections containing GFP-immunoreactive neurons were exposed to phosphate-buffered 1% osmium tetroxide for 1 hr, washed 4 × 5 min in distilled water and treated with 2% aqueous uranyl acetate for 30 min. After en bloc uranyl acetate staining, the sections were dehydrated in graded acetone solutions and propylene oxide, infiltrated with Durcupan resin (Fluka/Sigma), embedded on slides under coverslips cut from Aclar film (Electron Microscopy Sciences, Hatfield, PA) and polymerized for 2 days at 60°C.

To improve our ability to distinguish the dendritic architecture of GABAergic neurons in the superficial dorsal horn, we also embedded some of the GFP-stained longitudinal sections from the spinal cords of the GAD-GFP transgenic mice in resin. We processed these sections similarly to the sections for EM except that we omitted the osmication and en bloc staining with uranyl acetate. Although this protocol resulted in significant shrinkage of the sections and some fading of the peroxidase reaction product, tracking of the longitudinally oriented dendrites of heavily stained GAD-GFP neurons in the superficial dorsal horn of the transgenic mice was greatly facilitated.

For EM analysis of spinal cord sections containing MGE transplants, we cut out regions of the dorsal horn containing GFP-immunoreactive structures from the resin-embedded Vibratome sections. The majority of neuropil that we examined was in the region of the nucleus proprius (laminae III-V). Each region of interest was placed in a drop of fresh resin on top of a blank block, flattened under a glass coverslip and repolymerized for 48 hr. Blocks for EM analysis were trimmed and a diamond knife was used to cut silver to pale gold ultrathin sections from each block. Sections for conventional ultrastructural analysis were collected onto thin bar 300 mesh copper grids and stained with 2% aqueous uranyl acetate. Sections for post-embedding immunogold localization of GABA were collected onto nickel mesh grids.

Author Manuscript Author Manuscript Author Manuscript Author Manuscript

For light microscopic (LM) analysis, we examined immunostained sections from 1 of the mice with a short-term MGE transplant, from one of the mice with a long-term transplant and from the two GAD-GFP transgenic mice. Because the dendrites of GFP-positive cortical neurons from GAD-GFP transgenic mice were faintly stained after immunohistochemistry, we enhanced the peroxidase reaction product by osmication. Forebrain sections were dried onto chrome alum-gelatine coated slides, washed 2 × 5 min in distilled water and exposed to 0.05% aqueous OsO_4 for 15 min. After osmication, the sections received five quick rinses and 2 × 5 min washes in distilled water before air-drying, after which the sections were dehydrated and coverslipped with Permaslip mounting medium (Alban Scientific, St Louis, MO).

2.4 | Post-embedding immunogold staining for GABA

We localized GABA-immunoreactivity on ultrathin sections from two of the mice with short-term MGE transplants and one of the mice with a long-term transplant. The ultrathin sections were incubated in a solution containing 50 mM glycine, 75 mM NaCl in 50 mM sodium phosphate buffer, pH 7.3, for 20 mins and then rinsed several times with 150 mM NaCl in 20 mM phosphate buffer. To block non-specific antibody binding, grids were immersed for 30 min in blocking buffer, which contained 2% BSA-c (Aurion, Immuno Gold Reagents & Accessories, Wageningen, The Netherlands), 5% normal goat serum, 0.25% cold water fish skin gelatin, 10 mM Tris, 0.09% NaCl, 0.05% Triton X-100 and 0.05% thimerosal in 10 mM phosphate buffer, pH 7.3. Grids were then incubated overnight in a well-characterized rabbit polyclonal anti-GABA antiserum (Sigma; Table 1) diluted 1:1,000 with blocking buffer and subsequently washed for 10 min in blocking buffer followed by 3 × 5 min washes in phosphate-buffered saline (PBS). Next, we incubated the grids for 2 hr in goat anti-rabbit IgG conjugated to 10nm gold particles (Catalogue # 810.011, Aurion) diluted 1:30 with blocking buffer. After final washes in blocking buffer and PBS as above, the grids were dried and then examined in the electron microscope. All steps were done at room temperature.

2.5 | Data collection and analysis

Sections stained for LM were examined with an Olympus BX53F microscope fitted with UPLSAPO objectives. We obtained digital images of the sections with an Olympus DP72 camera and Olympus cellSens Entry version 1.6 software.

Ultrathin sections were examined and photographed with a JEOL 100CXII transmission electron microscope and a beam current of 80 kV. In sections from 5 of the 6 mice with short-term (5–6-week) transplants and from 2 of the mice with long-term (5–6-month) transplants, we counted synapses and direct contacts that MGE-derived GFP-immunoreactive neurons either made with unlabeled, presumptive host neurons or received from them. We recognize that an unlabeled profile may derive from transplanted MGE cells. However, given the complete penetration of immunoreagents that our immunocytochemical protocol produces, we believe that the great majority, if not all, unlabeled profiles are indeed host-derived. We classified a terminal apposing a GFP-immunoreactive cell body or dendrite as a synapse when vesicles were clustered pre-synaptically, a membrane specialization was present post-synaptically and/or there was a widened synaptic cleft. A terminal was

Author Manuscript Author Manuscript Author Manuscript Author Manuscript

classified as making a direct contact when vesicles were clustered pre-synaptically with neither a post-synaptic membrane specialization nor a widened synaptic cleft.

To avoid double counting, we assessed interactions between MGE-derived (GFP-positive) and host (GFP-negative) neurons in one ultrathin section from 1 to 3 blocks from each mouse. The blocks for counting contained the dorsal horn (usually laminae III–V) close to the center of the transplant, where the density of GFP-immunoreactive elements was highest. We focused on GFP-immunoreactive dendrites as these were the most commonly encountered structure derived from the transplanted MGE cells. In each mouse, we examined at least 70 GFP-immunostained dendrites and quantified the number of synapses or direct contacts that each received. In 2 of the mice with short-term transplants and in the two mice with long-term transplants, we estimated density of synaptic input by recording whether each dendrite received 1 or more synaptic inputs. We also counted synapses and direct contacts from unlabeled axons onto GFP-stained cell bodies as well as direct interactions between GFP-labeled axons and unlabeled dendrites, somata or axons.

2.6 | Figure preparation

Digital light and electron micrographs of GFP-immunoreactive structures were adjusted for sharpness, brightness and contrast using PhotoShop CS6, which was also used to prepare plates. The light microscopic images in Figure 1 are montages composed of 4 to 23 individual micrographs that were stitched together in PhotoShop.

3 | RESULTS

3.1 | Distribution of MGE-derived neurons in the spinal cord

All mice that received unilateral injections of GABAergic precursor transplants into the lumbar enlargement contained GFP-immunoreactive cells. Because of the placement of the injections, most of the GFP-labeled neurons were concentrated in ipsilateral laminae III–V. Labeled cells were also found in the superficial dorsal horn. We occasionally observed GFP-positive neurons in the white matter overlying the dorsal horn, particularly in areas close to the injection site. Rare GFP-labeled neurons migrated to the ventral horn, the contralateral dorsal horn or the dorsal columns.

3.2 | Morphology of MGE-derived neurons

In sections that were fixed and stained for EM and then mounted onto slides without osmication for viewing by LM (Figure 1), the transplanted neurons resembled cortical GABAergic neurons, with the majority having small round cell bodies and fine dendrites. This morphology was best appreciated in neurons that lay distant from the center of the MGE cell injection site, where transplanted neurons were more dispersed, and in deeper laminae of the dorsal horn (Figure 1b, f). In the superficial dorsal horn, the dendritic arbors of GFP-positive neurons appeared to be constrained by the boundaries of the grey matter (Figure 1b). Consistent with their cortical origin, the morphology of transplant-derived neurons (Figure 1b, f) resembled GFP-immunoreactive cortical neurons found in adult GAD-GFP transgenic mice (Figure 1g, h). In contrast, the morphology of MGE neurons transplanted into the spinal cord differed considerably from the intrinsic GFP-positive

Author Manuscript Author Manuscript Author Manuscript Author Manuscript

neurons in the spinal cord of the transgenic GAD-GFP mice. Consistent with previous observations (Todd, 2010), most GFP-labeled, GAD-expressing neurons in the superficial dorsal horn of the transgenic mice were fusiform with rostrocaudally oriented dendrites (Figure 1k, l) whereas in deeper laminae (Figure 1i, j) these neurons tended to be multipolar with a few primary dendrites that radiated circumferentially.

3.3 | Ultrastructure of MGE cell transplants

In mice with both short- and long-term transplants, GFP-positive neurons were readily identified by the black, electron dense immunoperoxidase reaction product in their nuclei as well as in their cytoplasm (Figure 2a, d). In single ultrathin sections, many of the neurons that originated from MGE cells contained large networks of rough endoplasmic reticulum and Golgi apparatus and had many mitochondria.

We observed GFP-immunoreactivity in vesicle-containing axon terminals, in lightly myelinated axons of small diameter (483 ± 37 nm, mean ± SD; $n = 6$) and in small diameter (~250 nm) presumptive intervaricose axonal segments (Figures 4–9). Most synaptic vesicles in transplant-derived terminals were small, round and clear. In lightly labeled terminals, we also found an occasional large dense-cored vesicle (Figures 4d, 9a), consistent with our previous observation that GABAergic MGE cells co-express neuropeptides (e.g., somatostatin J. M. Braz et al., 2012). Finally, in regions close to the injection site, we also observed GFP-immunoreactive somata and dendrites surrounded by glial processes, which we identified by the presence of many 10 nm filaments (Figures 3b, e, 4c, 5b). When glial processes were thin, 2–3 layers could surround a GFP-labeled soma or dendrite (e.g., Figure 3d). We presume that the abundance of glial elements near injection sites reflects gliosis due to the unavoidable transplant surgery-associated damage to the host.

3.4 | Synaptic input from the host to transplanted neurons

In mice with both short- and long-term transplants, MGE neurons received a rich synaptic input from presumptive host neurons (Figures 2–4). Although we found only a limited number of axosomatic inputs or direct contacts at short times post-transplant, host input to MGE-derived cell bodies (Figure 3) and dendrites (Figure 5) was more extensive in mice with long-term transplants. Although our analysis was limited to 2 mice with long-term transplants and thus our conclusions about long-term synaptic connectivity are preliminary, at all times posttransplantation, we encountered both symmetric (Figures 2c, 3f, 4b, d, 5b) and asymmetric (Figures 3c-e, 4a, c, d, 5) GFP-negative synapses onto transplanted cells and also many examples of the same unlabeled host terminal making a synapse/direct contact on both an MGE neuron and a host neuron (Figures 2e, 3f, 4b, d, 6b, 7a, 9g, h).

This initial qualitative analysis of host input onto the transplanted MGE cells suggested that the integration of the transplant into host circuits is dynamic. We quantified these changes in 5 mice with short-term transplants and in 2 mice with long-term transplants. Table 2 shows that, in the 5 mice with short-term (5–6-week) transplants, about half of the GFP-positive dendrites received a synapse or direct contact from an unlabeled host axon terminal. In the two mice with long-term (5–6-month) transplants, the proportion of GFP-labeled dendrites receiving GFP-negative (host) synaptic input was higher, close to 80%. Moreover, the

Author Manuscript Author Manuscript Author Manuscript Author Manuscript

number of dendrites that received input from 2 or more host terminals increased from 7 and 10% of all dendrites in 2 mice at 5–6 weeks post-transplantation to 20% and 50% in the 2 mice at 5–6 months after surgery. These data suggest that not only is there an increase in the number of dendrites that receive host inputs but also in the number of host inputs per dendrite. Taken together, these quantitative data show that host-transplant synaptic interactions evolve over time and specifically that there is a time-dependent increase in axodendritic and axosomatic input from the host to the MGE neurons.

3.5 | Synaptic output from transplanted neurons

3.5.1 | Transplant-on-host synapses—At both short and long times post-transplantation, we found synapses and direct contacts from the transplant onto the host, including axosomatic, axodendritic and occasional axoaxonic inputs (Figures 6–7). The majority of the axodendritic and axosomatic synaptic contacts were symmetric. There were also a few GFP-stained boutons that made synapses on spines that arose from unlabeled dendrites (Figure 7c) and some of these spines received a convergent synaptic input from the host.

In one of the mice with a long-term transplant, we sampled a large enough population of GFP-immunoreactive terminals in a single section so that we could quantify the synaptic targets of the MGE neurons. In this mouse, 53 of 78 (67.9%) GFP-labeled axon terminals directly contacted or synapsed on dendrites, almost all of which were small diameter. One of these GFP-positive terminals provided input to a spine. Thirteen (16.7%) MGE-derived terminals made a contact or synapse on a GFP-negative cell body and 6 (7.7%) made axoaxonic contacts with GFP-negative axon terminals. One of these axoaxonic contacts also directly apposed an adjacent GFP-negative cell body. We could not identify the synaptic target of the remaining 6 (7.7%) MGE-derived axons terminals.

3.5.2 | Transplant on transplant synapses—Remarkably, we also discovered that transplanted neurons occasionally provided synaptic input to other transplanted neurons (Figure 9e, f). All of the MGE-on-MGE synapses and direct contacts that we encountered were axodendritic.

3.5.3 | Transplants in synaptic glomeruli—In mice with short and long-term transplants, we identified a few GFP-immunoreactive dendrites and axon terminals that were part of synaptic glomeruli (Basbaum, Glazer, & Oertel, 1986; Ribeiro-da-Silva, Tagari, & Cuello, 1989), in which multiple terminals and dendrites of the GFP-negative host and GFP-positive transplant intermingled. In these glomeruli, we found examples of GFP-labeled MGE-derived dendrites post-synaptic to unlabeled (host) scalloped, central terminals, which are characteristic of primary afferents (Figure 8a). In one glomerulus, we observed an MGE-derived axon terminal in direct contact with an unlabeled scalloped terminal (Figure 8b). The absence of an intervening glial process suggests strongly that the MGE derived terminal is presynaptic to the host terminal.

Author Manuscript Author Manuscript Author Manuscript Author Manuscript

3.6 | Interaction between GABAergic host circuits and MGE transplants

In mice with both short- and long-term transplants, post-embedding immunogold staining to localize GABA-immunoreactivity allowed us to identify the neurotransmitter phenotype of lightly GFP-immunolabeled MGE-derived profiles (Figure 9). MGE terminals were GABA-gold labeled and formed synapses on unlabeled, presumptive host dendrites (Figure 9a, d) as well as direct contacts on GFP-negative axons (Figure 9b, g, h). These findings are consistent with our previous conclusion that the transplanted cells are indeed GABAergic. In addition, as expected, we found significant numbers of host terminals with GABA-gold labeling. Surprisingly, we observed GFP-negative, GABA-gold labeled terminals forming synapses on the dendrites (Figure 10a, b, d-f) and cell bodies (Figure 10a, c) of MGE cells. In other examples, there were direct contacts without a clear cut postsynaptic density (Figure 10e). This intrinsic inhibitory synaptic input to transplanted MGE neurons was present in mice with both short- (Figure 10a-e) and long-term transplants (Figure 10f). Finally, we found GABA-gold staining on MGE terminals that were presynaptic to MGE dendrites (Figure 9c, e, f). Taken together, these complex GABAergic synaptic relationships support our view that the integration of the transplants into the host circuitry is a random process, which can result in host inhibitory control of the transplanted cells.

4 | DISCUSSION

A major question concerning the ability of MGE transplants to ameliorate neurological dysfunction, from epilepsy to chronic pain and chronic itch, is whether the transplants integrate synaptically into host circuitry or whether they function as sophisticated, cell-based GABAergic pumps. We previously suggested that integration of the transplanted MGE cells into host circuitry is, in fact, an essential component of the antihyperalgesic and antipruritic effects of the transplants (J. M. Braz et al., 2012, 2014, 2015). Our conclusions were based on the transneuronal transfer of lectins and viral tracers as well as Fos induction in the transplants in response to noxious and innocuous hindpaw stimulation of the host. Although the present analysis was performed in uninjured mice, which presumably did not have the GABAergic dysfunction characteristic of mice with a peripheral nerve injury, we nevertheless provide strong evidence that there is remarkable synaptic integration of transplanted cells into host dorsal horn circuitry. Furthermore, the connectivity between the transplant and host is neither static, nor short-lived, but rather involves ongoing, dynamic circuit reorganization. In fact, synaptic contacts from the host onto transplant-derived neurons increased significantly over the 6-month observation period, roughly equivalent to one-quarter of the mouse lifespan. Importantly, double labeling for GFP and GABA confirmed that the MGE cells contain the inhibitory neurotransmitter GABA. Taken together with our previous demonstration of the critical contribution of GABA to the recovery of function, we conclude that GABA release at synapses made by MGE cells is an essential component of the therapeutic effects of the transplants.

4.1 | Complexity of the synaptic integration of transplanted MGE cells

The synaptic reorganization that we report here is heterogeneous and involves extensive interactions between MGE cells and local circuit neurons and primary afferent terminals in the dorsal horn. We found synaptic contacts from scalloped terminals onto MGE-derived,

Author Manuscript Author Manuscript Author Manuscript Author Manuscript

GFP-positive dendrites. These contacts involved multiple, unlabeled dendrites, a glomerular synaptic assembly characteristic of primary afferent terminals (Basbaum et al., 1986; Ribeiro-da-Silva et al., 1989). This ultrastructural arrangement is consistent with our recent finding that optogenetic stimulation of TRPV1-expressing, unmyelinated afferents monosynaptically activates transplanted cells (Etlin et al., 2016). Conversely, we also observed axoaxonic appositions between MGE and presumptive host terminals, including a GFP-immunoreactive terminal that likely formed a synapse onto a scalloped terminal at the center of a synaptic glomerulus. Although a clear postsynaptic density was not apparent, this synaptic arrangement is characteristic of the structural basis for presynaptic inhibition of primary afferents by GABAergic inputs (Basbaum et al., 1986).

Of particular note is the complexity of the GABAergic inhibitory circuits engaged by the MGE cells. For example, in our double labeling study, we observed GFP-negative, GABA-labeled terminals synapsing onto MGE processes that were labeled for both GFP and GABA. We presume that the host GABAergic interneurons provide most of this presynaptic GABAergic input to the MGE cells, although some synapses may also derive from spinally projecting GABAergic neurons in the medulla (Cho & Basbaum, 1991; Francois et al., 2017). Regardless of the origin of the inputs to the MGE cells, these complex synaptic relationships demonstrate that the transplants, in addition to being activated by primary afferents, are also under inhibitory control (feedback inhibition) from local host circuitry. We suggest that these connections are part of a GABA-stat circuit that maintains the transplant's endogenous inhibitory tone at levels that are normal for the host spinal cord. In agreement with this hypothesis, MGE cells normalize GAD mRNA levels and have no effect on baseline mechanical thresholds when transplanted into uninjured mice (J. M. Braz et al., 2012). Because intrathecal injections of GABA agonists reliably increase baseline GABA thresholds (Kaneko & Hammond, 1997), our findings argue strongly that the transplants do not act as a pump that continuously releases GABA. Interestingly, we also found synaptic interactions between transplanted cells, which provide yet another source of inhibitory control. The presence of MGE-on-MGE synapses strongly supports our earlier contention that integration of the transplants into host dorsal horn circuitry is random. For this reason, we do not believe that the transplants follow a developmental program that recapitulates the endogenous GABAergic inhibitory circuits. Rather than being guided by specific neurotrophic signals, as occurs during development, we suggest that synaptic connections develop as a result of proximity of transplanted cells and host neurons. This conclusion is consistent with our previous finding that the number of transplanted cells does not correlate with the magnitude of the functional recovery but relates more to the extensive axonal and dendritic outgrowth of individual transplanted cells throughout the dorsal horn.

4.2 | Structural plasticity of the adult spinal cord

Numerous anatomical and electrophysiological studies have demonstrated reorganization of the central nervous system after brain injury (Emery, Royo, Fischer, Saatman, & McIntosh, 2003; Young, 2014), including the ability of transplants to re-innervate denervated neurons (Raisman & Field, 1990; Schwab, 2002). In those studies, however, the magnitude of the regenerative plasticity was limited and likely short-lived (J. Silver, Schwab, & Popovich, 2015). In contrast, the long-term, transplant-mediated recovery of function that we observed

Author Manuscript Author Manuscript Author Manuscript Author Manuscript

in models of neuropathic pain and itch presumably reflects persistent collateral sprouting and synaptic plasticity between the host and transplant. The ability of the MGE transplants to form new synapses in the spinal cord can, in part, be attributed to their embryonic derivation, which endows them with a high intrinsic capacity for growth (Baraban et al., 2009; Goslin, Schreyer, Skene, & Banker, 1990; Thompson, Grealish, Kirik, & Bjorklund, 2009). On the other hand, the anatomical and functional synaptic connections from the host to the transplant also provide excellent examples of structural plasticity, that is, axonal growth and synaptic reorganization of uninjured host neurons (Holtmaat & Svoboda, 2009; Merzenich, Van Vleet, & Nahum, 2014; Sirevaag & Greenough, 1988).

Although structural plasticity reportedly can occur in association with learning and experience, where it is undoubtedly beneficial, there are few reports of behavioral manifestations of structural plasticity in the absence of significant injury. We appreciate that de novo synapse formation with the transplanted cells did not occur in a completely normal spinal cord because the transplant needle undoubtedly produced some damage. Nevertheless, comparable injury in the cortex produced very limited sprouting (Blizzard et al., 2011). Furthermore, although biochemical consequences of the injury may facilitate growth by host neurons, most studies emphasize the plethora of inhibitory factors associated with CNS injury, including astrocytic scars and growth-inhibiting molecules, such as semaphorins and chondroitin sulfate proteoglycans (Fawcett, 2015; D. J. Silver & Silver, 2014; J. Silver et al., 2015; Sun & He, 2010). Taken together with the fact that transplants performed in uninjured spinal cord can prevent the mechanical hypersensitivity produced by subsequent nerve injury (Etlin et al., 2016), our demonstration of extensive synaptic reorganization in the largely intact spinal cord provides some of the most powerful evidence that structural plasticity in the adult spinal cord can have significant behavioral consequences.

The structural plasticity that we observed is particularly impressive given that the normal environment of the transplanted cells is the cerebral cortex and that the cells appear to retain their cortical phenotypes. Specifically, the MGE cells express somatostatin (J. M. Braz et al., 2012; Etlin et al., 2016), which is characteristic of some cortical, but not spinal cord, GABAergic interneurons. In the present report we also demonstrate that the morphology of the transplanted cells is comparable to cortical GAD-GFP interneurons in transgenic GAD-GFP mice, with round cell bodies and widely ramifying dendrites. Importantly, we found that synaptic reorganization was not limited to the transplanted MGE cell body, which most commonly was located in the deep dorsal horn, but also occurred in relation to transplant-derived dendrites and axons that arborized hundreds of micrometers from their MGE cell bodies of origin.

Finally, our hypothesis that transplant integration establishes a GABAstat that is somehow sensitive to intrinsic levels of GABA within the host dorsal horn and adjusts inhibitory control to a level that maintains normal baseline mechanical thresholds has interesting parallels with a proposal from the structural plasticity literature. Specifically, some forms of experience-dependent structural plasticity, notably the de novo formation of multisynaptic boutons, serves to regulate neural network homeostasis in the mammalian cortex (Holtmaat & Svoboda, 2009). The presence of spinal cord terminals that form synapses with both transplant and host dendrites suggests that comparable forms of structural plasticity occur

Author Manuscript Author Manuscript Author Manuscript Author Manuscript

not only in response to experience but also after transplantation of embryonic cells into the normal, intact adult spinal cord.

ACKNOWLEDGMENTS

We thank Larry Ackerman for help with ultrathin sectioning and post-embedding immunogold staining for GABA. This work was funded by grants to JMB (NIH # NS078326) and AIB (NIH # R35NS097306)

Funding information

Grant Sponsor: National Institute of Neurological Disorders and Stroke, Grant Nos. NS078326, R35NS097306

REFERENCES

Baraban SC, Southwell DG, Estrada RC, Jones DL, Sebe JY, Alfaro-Cervello C, … Alvarez-Buylla A (2009). Reduction of seizures by transplantation of cortical GABAergic interneuron precursors into Kv1.1 mutant mice. Proceedings of the National Academy of Sciences of the United States of America, 106(36), 15472–15477. https://doi.org/10.1073/pnas.0900141106 [PubMed: 19706400]

Basbaum AI, Glazer EJ, & Oertel W (1986). Immunoreactive glutamic acid decarboxylase in the trigeminal nucleus caudalis of the cat: A light- and electron-microscopic analysis. Somatosensory Research, 4(1), 77–94. [PubMed: 3541116]

Blizzard CA, Chuckowree JA, King AE, Hosie KA, McCormack GH, Chapman JA, … Dickson TC (2011). Focal damage to the adult rat neocortex induces wound healing accompanied by axonal sprouting and dendritic structural plasticity. Cerebral Cortex, 21(2), 281–291. https://doi.org/10.1093/cercor/bhq091 [PubMed: 20511339]

Braz J, Solorzano C, Wang X, & Basbaum AI (2014). Transmitting pain and itch messages: A contemporary view of the spinal cord circuits that generate gate control. Neuron, 82(3), 522–536. https://doi.org/10.1016/j.neuron.2014.01.018 [PubMed: 24811377]

Braz JM, Juarez-Salinas D, Ross SE, & Basbaum AI (2014). Transplant restoration of spinal cord inhibitory controls ameliorates neuropathic itch. Journal of Clinical Investigation, 124(8), 3612–3616. https://doi.org/10.1172/JCI75214 [PubMed: 25003193]

Braz JM, Sharif-Naeini R, Vogt D, Kriegstein A, Alvarez-Buylla A, Rubenstein JL, & Basbaum AI (2012). Forebrain GABAergic neuron precursors integrate into adult spinal cord and reduce injury-induced neuropathic pain. Neuron, 74(4), 663–675. https://doi.org/10.1016/j.neuron.2012.02.033 [PubMed: 22632725]

Braz JM, Wang X, Guan Z, Rubenstein JL, & Basbaum AI (2015). Transplant-mediated enhancement of spinal cord GABAergic inhibition reverses paclitaxel-induced mechanical and heat hypersensitivity. Pain, 156(6), 1084–1091. https://doi.org/10.1097/j.pain.0000000000000152 [PubMed: 25760475]

Cho HJ, & Basbaum AI (1991). GABAergic circuitry in the rostral ventral medulla of the rat and its relationship to descending antinociceptive controls. The Journal of Comparative Neurology, 303(2), 316–328. https://doi.org/10.1002/cne.903030212 [PubMed: 2013643]

Coull JA, Beggs S, Boudreau D, Boivin D, Tsuda M, Inoue K, … De Koninck Y (2005). BDNF from microglia causes the shift in neuronal anion gradient underlying neuropathic pain. Nature, 438(7070), 1017–1021. https://doi.org/10.1038/nature04223 [PubMed: 16355225]

Emery DL, Royo NC, Fischer I, Saatman KE, & McIntosh TK (2003). Plasticity following injury to the adult central nervous system: Is recapitulation of a developmental state worth promoting? Journal of Neurotrauma, 20(12), 1271–1292. https://doi.org/10.1089/089771503322686085 [PubMed: 14748977]

Etlin A, Braz JM, Kuhn JA, Wang X, Hamel KA, Llewellyn-Smith IJ, & Basbaum AI (2016). Functional synaptic integration of forebrain GABAergic precursors into the adult spinal cord. The Journal of Neuroscience, 36(46), 11634–11645. https://doi.org/10.1523/JNEUROSCI.2301-16.2016 [PubMed: 27852772]

Author Manuscript Author Manuscript Author Manuscript Author Manuscript

Fawcett JW (2015). The extracellular matrix in plasticity and regeneration after CNS injury and neurodegenerative disease. Progress in Brain Research, 218, 213–226. https://doi.org/10.1016/bs.pbr.2015.02.001 [PubMed: 25890139]

Francois A, Low SA, Sypek EI, Christensen AJ, Sotoudeh C, Beier KT, … Scherrer G (2017). A brainstem-spinal cord inhibitory circuit for mechanical pain modulation by GABA and enkephalins. Neuron, 93(4), 822–839. e826 https://doi.org/10.1016/j.neuron.2017.01.008 [PubMed: 28162807]

Fukuoka T, Tokunaga A, Kondo E, Miki K, Tachibana T, & Noguchi K (1998). Change in mRNAs for neuropeptides and the GABA(A) receptor in dorsal root ganglion neurons in a rat experimental neuropathic pain model. Pain, 78(1), 13–26. https://doi.org/S0304-3959(98)00111-0 [pii] [PubMed: 9822208]

Goslin K, Schreyer DJ, Skene JH, & Banker G (1990). Changes in the distribution of GAP-43 during the development of neuronal polarity. Journal of Neuroscience, 10(2), 588–602. [PubMed: 2137532]

Holtmaat A, & Svoboda K (2009). Experience-dependent structural synaptic plasticity in the mammalian brain. Nature Reviews Neuroscience, 10(9), 647–658. https://doi.org/10.1038/nrn2699 [PubMed: 19693029]

Kaneko M, & Hammond DL (1997). Role of spinal gammaaminobutyric acidA receptors in formalin-induced nociception in the rat. Journal of Pharmacology and Experimental Therapeutics, 282(2), 928–938. [PubMed: 9262360]

Llewellyn-Smith IJ, Dicarlo SE, Collins HL, & Keast JR (2005). Enkephalin-immunoreactive interneurons extensively innervate sympathetic preganglionic neurons regulating the pelvic viscera. The Journal of Comparative Neurology, 488(3), 278–289. https://doi.org/10.1002/cne.20552 [PubMed: 15952166]

Llewellyn-Smith IJ, Martin CL, Fenwick NM, Dicarlo SE, Lujan HL, & Schreihofer AM (2007). VGLUT1 and VGLUT2 innervation in autonomic regions of intact and transected rat spinal cord. The Journal of Comparative Neurology, 503(6), 741–767. https://doi.org/10.1002/cne.21414 [PubMed: 17570127]

Llewellyn-Smith IJ, & Minson JB (1992). Complete penetration of antibodies into vibratome sections after glutaraldehyde fixation and ethanol treatment: Light and electron microscopy for neuropeptides. Journal of Histochemistry & Cytochemistry, 40(11), 1741–1749. https://doi.org/10.1177/40.11.1431060 [PubMed: 1431060]

Llewellyn-Smith IJ, Reimann F, Gribble FM, & Trapp S (2011). Preproglucagon neurons project widely to autonomic control areas in the mouse brain. Neuroscience, 180, 111–121. https://doi.org/10.1016/j.neuroscience.2011.02.023 [PubMed: 21329743]

Merzenich MM, Van Vleet TM, & Nahum M (2014). Brain plasticity-based therapeutics. Frontiers in Human Neuroscience, 8, 385 https://doi.org/10.3389/fnhum.2014.00385 [PubMed: 25018719]

Moore KA, Kohno T, Karchewski LA, Scholz J, Baba H, & Woolf CJ (2002). Partial peripheral nerve injury promotes a selective loss of GABAergic inhibition in the superficial dorsal horn of the spinal cord. Journal of Neuroscience, 22(15), 6724–6731. https://doi.org/20026611 [PubMed: 12151551]

Raisman G, & Field PM (1990). Synapse formation in the adult brain after lesions and after transplantation of embryonic tissue. Journal of Experimental Biology, 153, 277–287. [PubMed: 2280225]

Ribeiro-da-Silva A, Tagari P, & Cuello AC (1989). Morphological characterization of substance P-like immunoreactive glomeruli in the superficial dorsal horn of the rat spinal cord and trigeminal subnucleus caudalis: A quantitative study. The Journal of Comparative Neurology, 281(4), 497–415. https://doi.org/10.1002/cne.902810402 [PubMed: 2468697]

Schwab ME (2002). Increasing plasticity and functional recovery of the lesioned spinal cord. Progress in Brain Research, 137, 351–359. https://doi.org/10.1016/S0079-6123(02)37026-2 [PubMed: 12440377]

Silver DJ, & Silver J (2014). Contributions of chondroitin sulfate proteoglycans to neurodevelopment, injury, and cancer. Current Opinion in Neurobiology, 27, 171–178. https://doi.org/10.1016/j.conb.2014.03.016 [PubMed: 24762654]

Author Manuscript Author Manuscript Author Manuscript Author Manuscript

Silver J, Schwab ME, & Popovich PG (2015). Central nervous system regenerative failure: Role of oligodendrocytes, astrocytes, and microglia. Cold Spring Harbor Perspectives in Biology, 7(3), a020602 https://doi.org/10.1101/cshperspect.a020602

Sirevaag AM, & Greenough WT (1988). A multivariate statistical summary of synaptic plasticity measures in rats exposed to complex, social and individual environments. Brain Research, 441(1-2), 386–392. https://doi.org/10.1016/0006-8993(88)91420-5 [PubMed: 3359241]

Sun F, & He Z (2010). Neuronal intrinsic barriers for axon regeneration in the adult CNS. Current Opinion in Neurobiology, 20(4), 510–518. https://doi.org/10.1016/j.conb.2010.03.013 [PubMed: 20418094]

Tamamaki N, Yanagawa Y, Tomioka R, Miyazaki J, Obata K, &Kaneko T (2003). Green fluorescent protein expression and colocalization with calretinin, parvalbumin, and somatostatin in the GAD67-GFP knock-in mouse. The Journal of Comparative Neurology, 467(1), 60–79. https://doi.org/10.1002/cne.10905 [PubMed: 14574680]

Thompson LH, Grealish S, Kirik D, & Bjorklund A (2009). Reconstruction of the nigrostriatal dopamine pathway in the adult mouse brain. European Journal of Neuroscience, 30(4), 625–638. https://doi.org/10.1111/j.1460-9568.2009.06878.x [PubMed: 19674082]

Todd AJ (2010). Neuronal circuitry for pain processing in the dorsal horn. Nature Reviews Neuroscience, 11(12), 823–836. https://doi.org/10.1038/nrn2947 [PubMed: 21068766]

Young W (2014). Spinal cord regeneration. Cell Transplantation, 23(4–5), 573–611. https://doi.org/10.3727/096368914X678427 [PubMed: 24816452]

Author Manuscript Author Manuscript Author Manuscript Author Manuscript

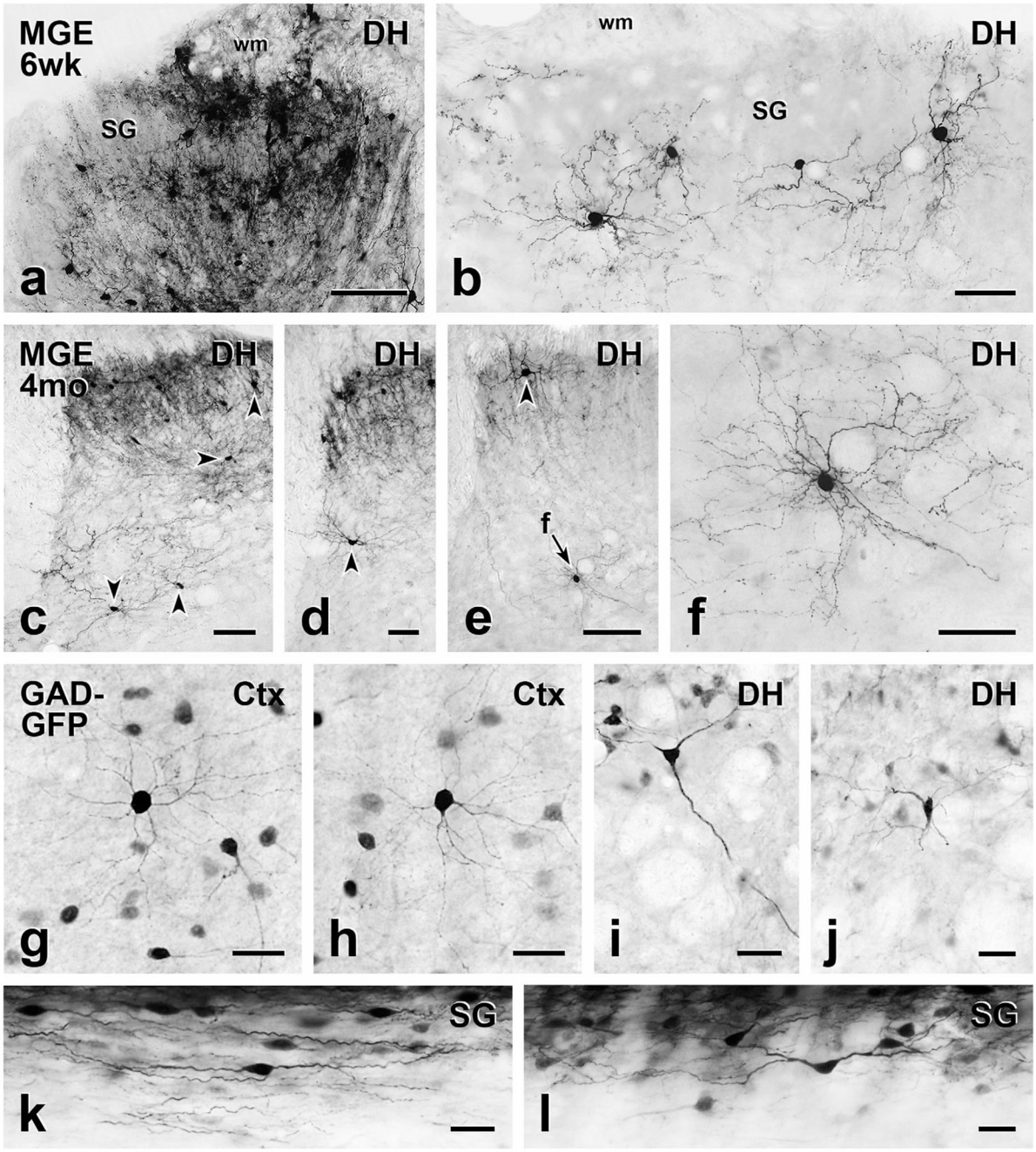

FIGURE 1.

Comparison of short- and long-term MGE cell morphology with cortical and spinal cord neurons from GAD-GFP transgenic mice. (a) At the level of the injection site, MGE-derived, GFP-immunoreactive cell bodies and processes are densely distributed throughout the dorsal horn (DH) 6 weeks post-transplantation. SG, substantia gelatinosa; wm, white matter. (b) Morphology of the MGE cells that migrated from the injection site is readily appreciated. They have small round or oval cell bodies with many fine dendrites, which are characteristics of cortical (Ctx) GABAergic interneurons (g & h). (c–f) Five months after

Author Manuscript Author Manuscript Author Manuscript Author Manuscript

transplantation, the MGE cells retain their cortical morphology. Arrowheads point to cell bodies of MGE neurons. Arrow F in E points to a cell shown at higher magnification in F. (g–l) Compared to cortical GAD-GFP neurons from transgenic GAD-GFP mice (g & h), those in deeper dorsal horn (i & j) are generally multipolar with a few primary dendrites that radiate circumferentially. Longitudinal sections (k & l) revealed that transgenic GAD-GFP neurons in the SG have a characteristic islet cell morphology, with fusiform cell bodies and rostrocaudally oriented dendrites. Scale bars: 100 μm in (a) and (c); 50 μm in (b), (d-f); 25 μm in (g-l)

Author Manuscript Author Manuscript Author Manuscript Author Manuscript

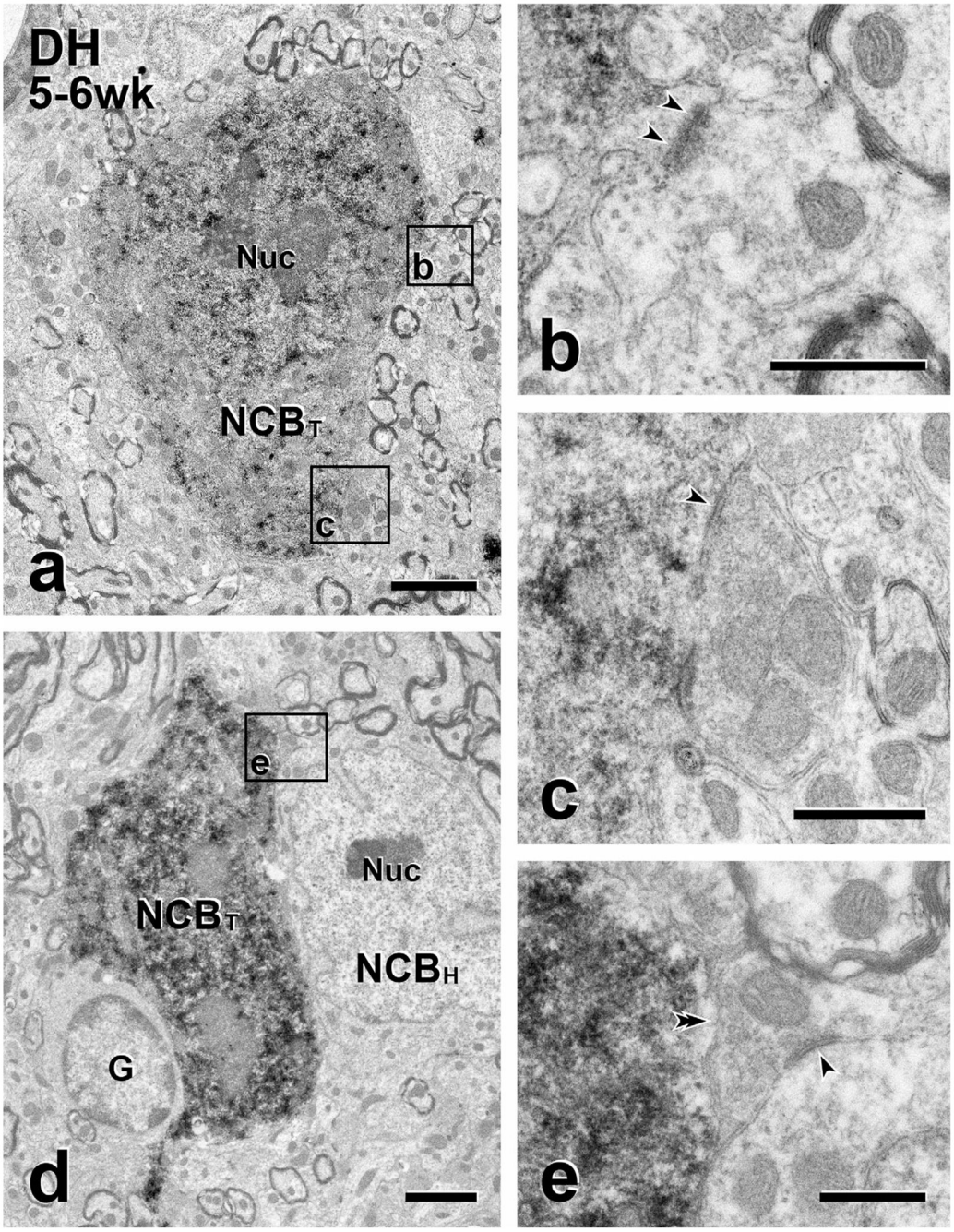

FIGURE 2.

Short-term transplants: presynaptic inputs from the host to transplant cell bodies. (a & d) Immunoperoxidase reaction product identifies GFP-immunoreactive transplant cell bodies (NCB_T) in the dorsal horn (DH). Boxed areas in (a) (Boxes b, c) and in (d) (Box e) illustrate unlabeled (host) axon terminals presynaptic (arrowheads) to GFP-labeled transplant cell bodies. In (a), the transplant cell body receives both an asymmetric and a symmetric synapse. The density postsynaptic to the unlabeled terminal in (b) is thick (i.e., an asymmetric synapse) whereas the density postsynaptic to the unlabeled terminal in (c) is thin

Author Manuscript Author Manuscript Author Manuscript Author Manuscript

(i.e., a symmetric synapse). In (d), the cell body of a GFP-negative (host) neuron (NCB_H) and a glial cell (G) abut the GFP-positive transplanted cell body. (e) The unlabeled axon terminal in (e) directly contacts (double arrowhead) the GFP-positive cell body in (d), without an intervening glia process and also forms a symmetric synapse (arrowheads) with an unlabeled host cell body. Nuc, neuronal nucleus. Scale bars: 2 μm in (a, d); 500 nm in (b, c, e)

Author Manuscript Author Manuscript Author Manuscript Author Manuscript

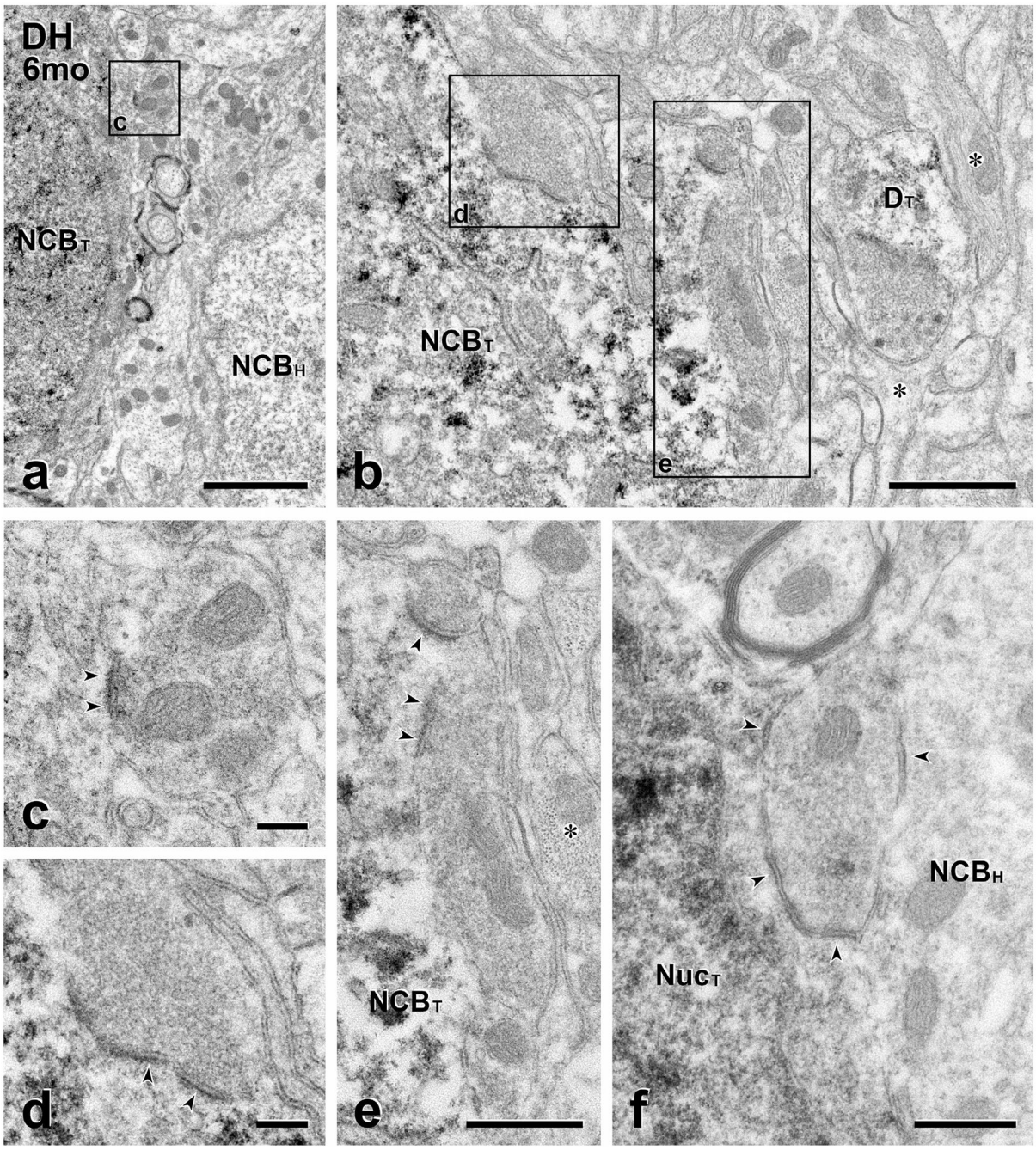

FIGURE 3.

Long-term transplants: Presynaptic inputs from the host to transplant cell bodies. (a & b) In (a), the GFP-positive cell body of a transplanted neuron (NCB_T) lies close to the unlabeled cell body of a host neuron (NCB_H). In (b), a transplant cell body (NCB_T) is located near the center of the injection site, where there are many glial processes (*) that are full of 10 nm filaments. Boxed area (c) in (a) and boxed areas (d) and (e) in (b) are shown at higher magnification in panels (c–e), respectively. D_T, dendrite of a transplanted neuron. (c–e) Unlabeled host axon terminals (c, d) and (e) synapse (arrowheads) on the GFP-positive cell

Author Manuscript Author Manuscript Author Manuscript Author Manuscript

bodies in (a) and (b). Note presynaptic clustering of vesicles and asymmetric synapses. (f) This unlabeled host axon terminal is presynaptic (arrowheads) to both an unlabeled host and a GFP-labeled transplant cell body. Nuc_T, nucleus of a transplanted neuron. Scale bars: 2 μm in (a); 1 μm in (b); 500 nm in (c–f)

Author Manuscript Author Manuscript Author Manuscript Author Manuscript

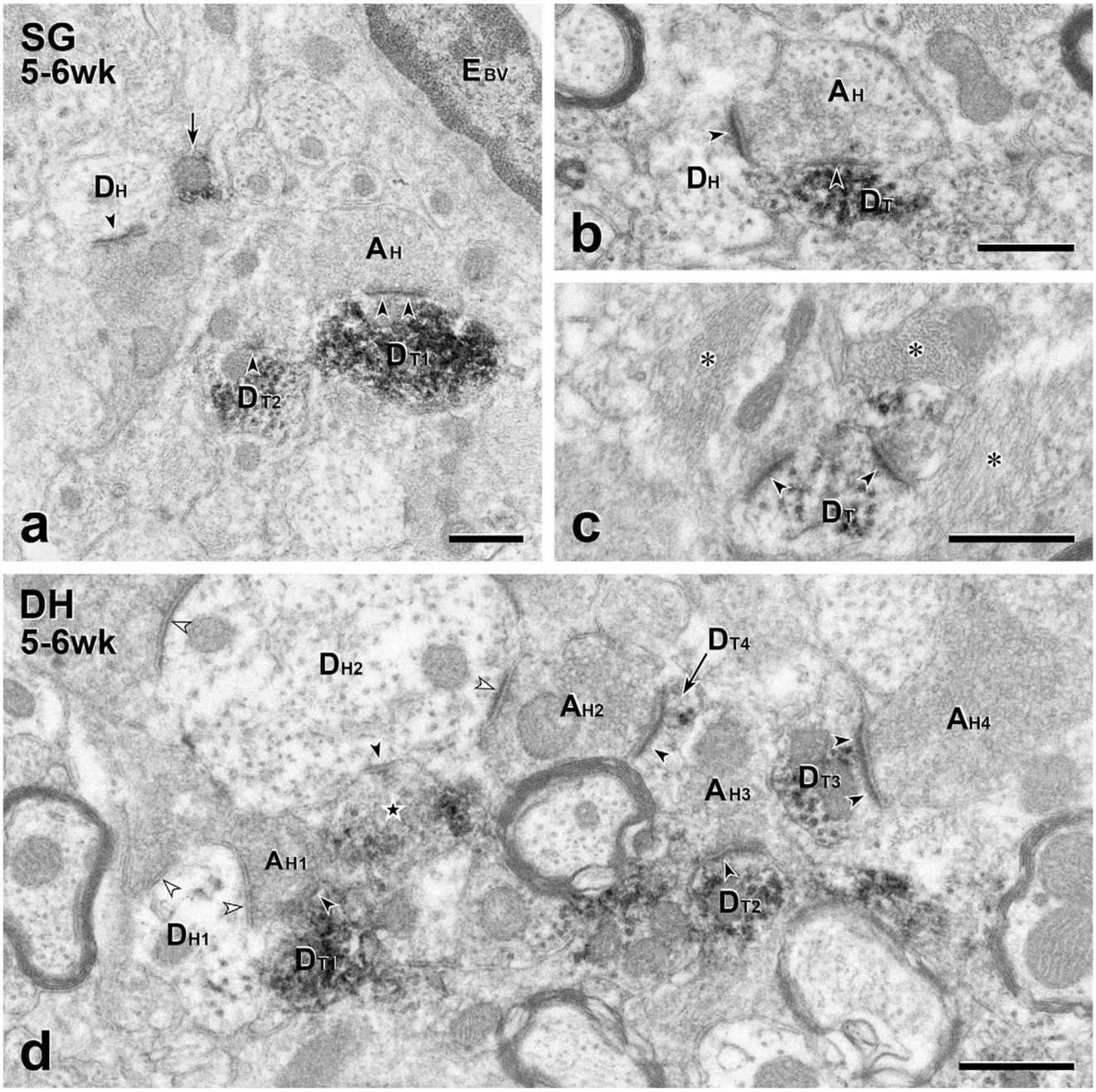

FIGURE 4.

Short term transplants: Presynaptic inputs from the host to transplant dendrites. (a–c) In the substantia gelatinosa (SG), unlabeled host terminals (A_H) are presynaptic (arrowheads) to GFP-immunoreactive transplant dendrites (D_T). In (a), the unlabeled synapse on D_{T1} is asymmetric. A nearby unlabeled host dendrite (D_H) also receives an asymmetric synapse (arrowhead). The arrow points to a likely intervaricose segment of a transplant axon, a GFP-positive profile common in the SG. E_{BV}, endothelial cell of a blood vessel. (b) A GFP-immunoreactive dendrite (D_T) receives a symmetric synapse (arrowheads) from an unlabeled host terminal (A_H) that also forms an asymmetric synapse (arrowhead) with an

Author Manuscript Author Manuscript Author Manuscript Author Manuscript

unlabeled host dendrite (D_H). (c) Two unlabeled host terminals form asymmetric synapses (arrowheads) on a GFP-positive MGE-derived dendrite (D_T). The area shown contains many glial processes (asterisks). (d) This 10.45 μm^2 field in deeper dorsal horn (DH) illustrates the density and complexity of MGE-derived synaptic connections. Four GFP-positive dendrites ($D_{T1–4}$) receive synapses from unlabeled host axon terminals ($A_{H1–4}$). The field also includes a GFP-immunoreactive transplant-derived axon terminal (star) that is presynaptic to an unlabeled host dendrite (D_{H2}). D_{H2} receives convergent input from two unlabeled host terminals, one of which (A_{H2}) is also presynaptic to a GFP-labeled transplant dendrite (D_{T4}). Black arrowheads, synapses in which MGE neurons are pre- or postsynaptic; white arrowheads, synapses involving only host neurons. Scale bars: 500 nm in (a–d)

Author Manuscript Author Manuscript Author Manuscript Author Manuscript

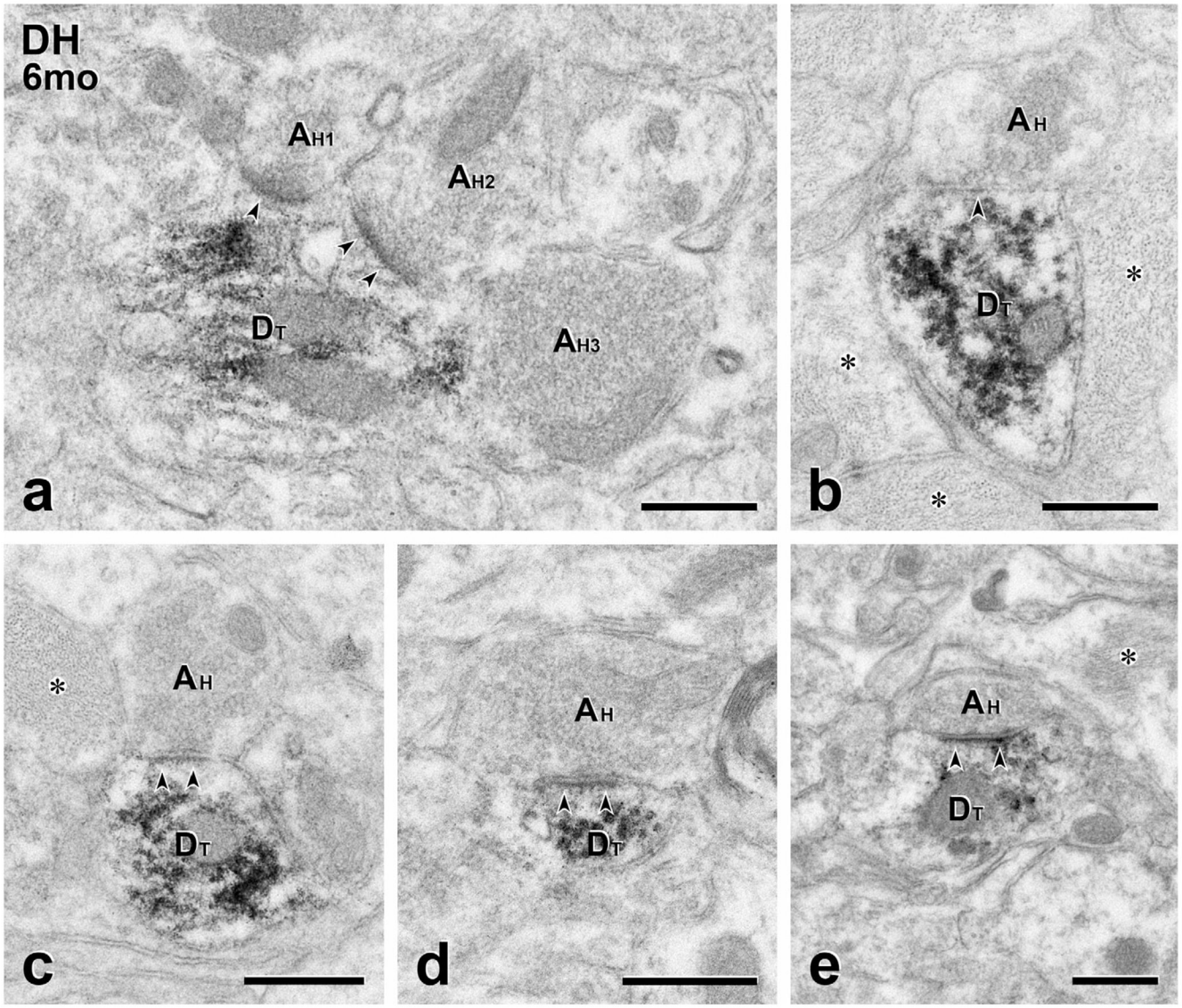

FIGURE 5.

Long term transplants: presynaptic inputs from the host to transplant dendrites. (a) Two unlabeled host terminals (A_{H1}, A_{H2}) converge (arrowheads) on a large GFP-labeled transplant-derived dendrite (D_T), forming symmetric synapses. There is also likely input from a third host terminal (A_{H3}). (b–e) Both asymmetric (b) and asymmetric (c–e) synaptic specializations (arrowheads) are found between GFP-negative host axon terminals (A_H) and GFP-positive transplant dendrites (D_T). Scale bars: 500 nm in (a–e)

Author Manuscript Author Manuscript Author Manuscript Author Manuscript

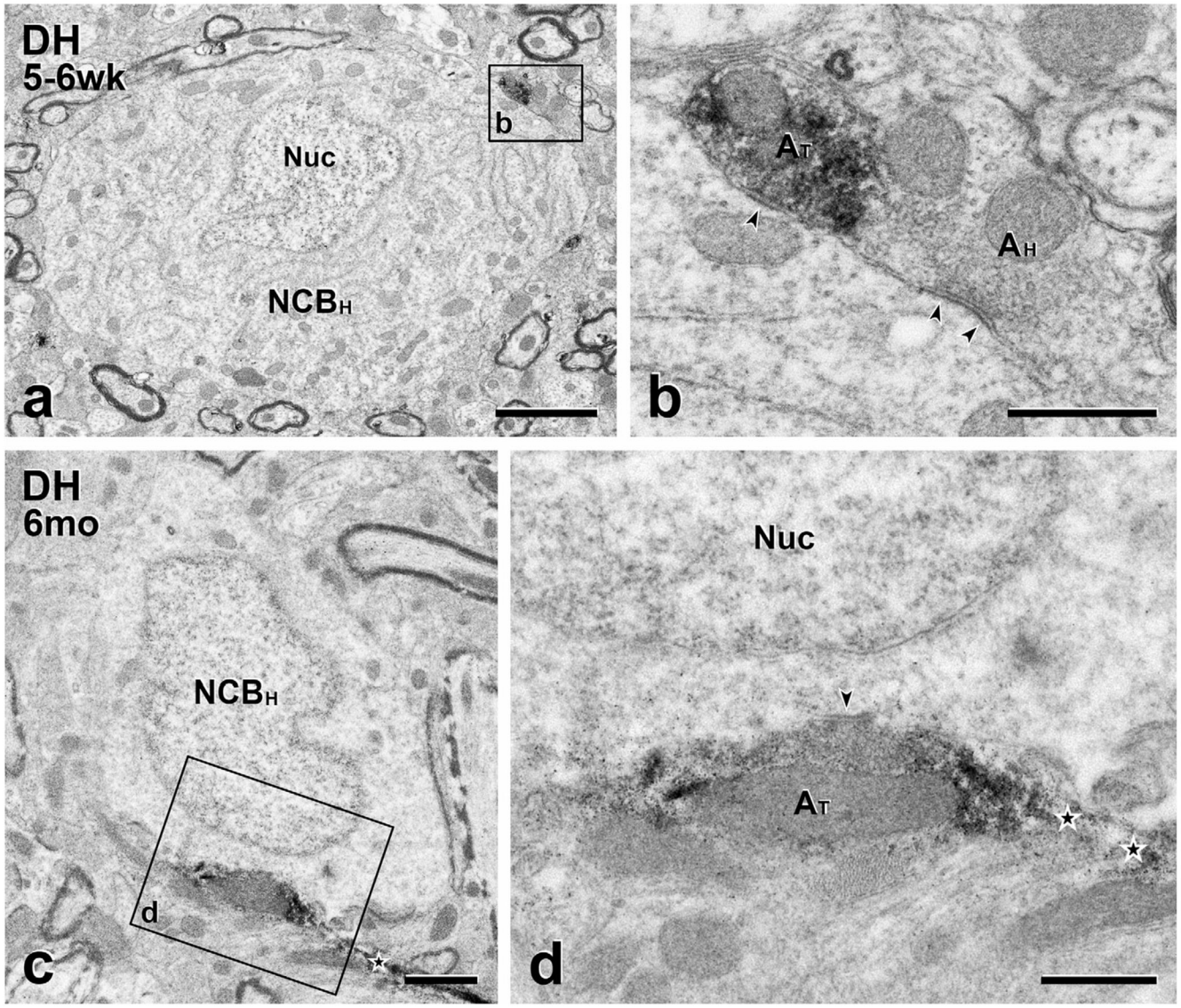

FIGURE 6.

Short- and long-term transplants: MGE-derived axons are presynaptic to host cell bodies. GFP-immunoreactive transplant-derived terminals (A_T) form synapses (arrowheads) on the unlabeled cell bodies of host neurons (NCB_H). (a & c), Low magnification micrographs of host neuronal cell bodies after short (a) and long-term (c) transplantation. The transplant-derived (symmetric) synapses (boxed areas b and d in a and c) are magnified (A_T; arrowheads) in panels (b) and (d), respectively. The terminal in (d) is continuous with one of its intervaricose segments (star). In (b), the adjacent host terminal (A_H) synapses on the host cell body and directly contacts the transplant-derived terminal. Nuc, neuronal nucleus. Scale bars: 2 μm in (a); 1 μm in (c); 500 nm in (c) and (d)

Author Manuscript Author Manuscript Author Manuscript Author Manuscript

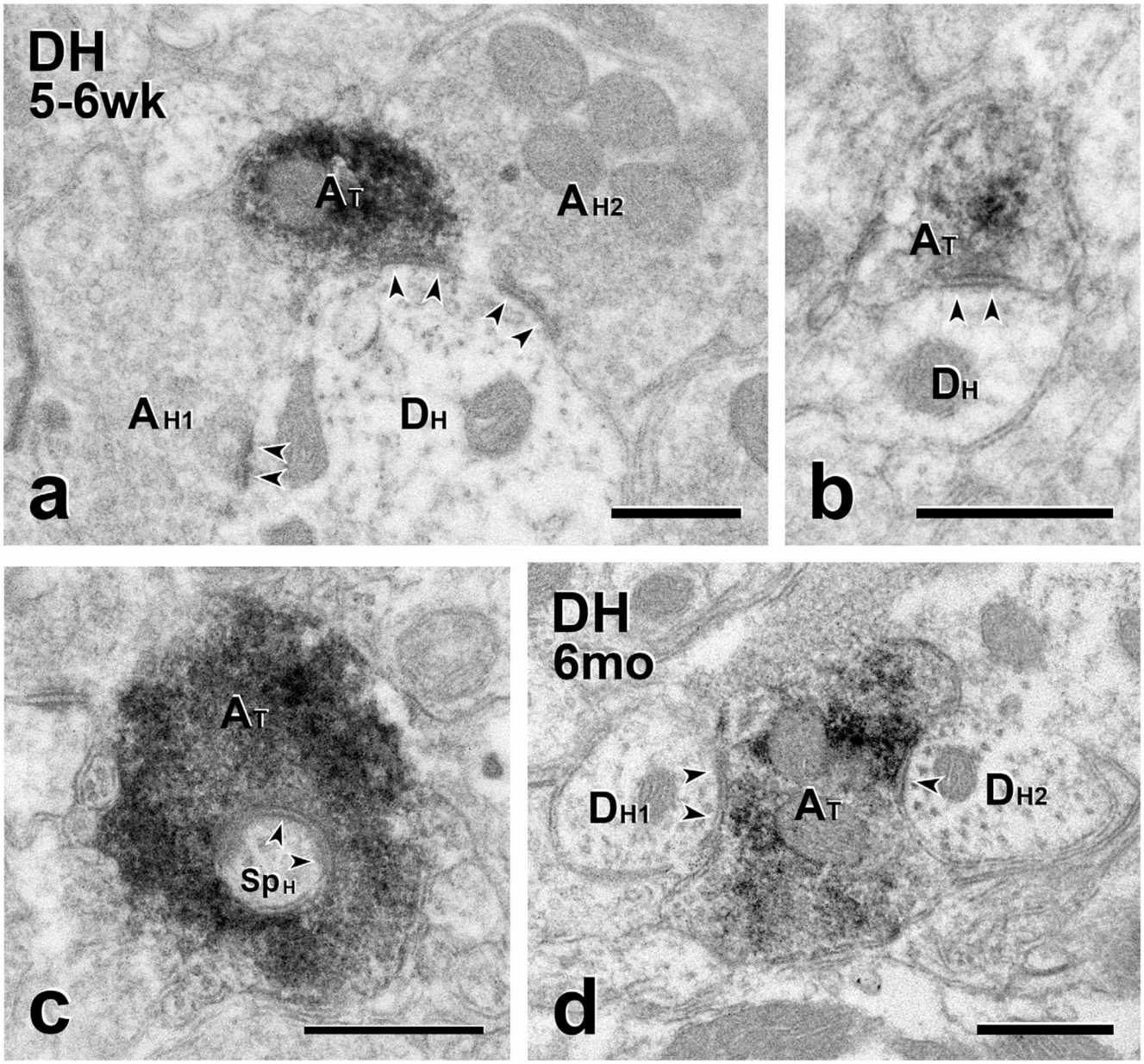

FIGURE 7.

Short- and long-term transplants: MGE-derived axons are presynaptic to host dendrites. (a–e) Short-term transplants. (a) A GFP–immunoreactive transplant-derived terminal (A_T) makes a symmetric synapse (arrowheads) with an unlabeled host dendrite (D_H) that is also postsynaptic to two unlabeled host-derived terminals (A_{H1} and A_{H2}). (b) GFP-labeled transplant terminal (A_T) forming a symmetric synapse on an unlabeled host dendrite (D_H). (c) A GFP-labeled transplant terminal (A_T) that is presynaptic to a spine arising from an unlabeled host neuron (Sp_H). (d) Long-term transplant. Two unlabeled host dendrites (D_{H1} and D_{H2}) receive symmetric synapses from the same GFP-immunoreactive transplant-derived axon terminal (A_T). Scale bars: 500 nm

Author Manuscript Author Manuscript Author Manuscript Author Manuscript

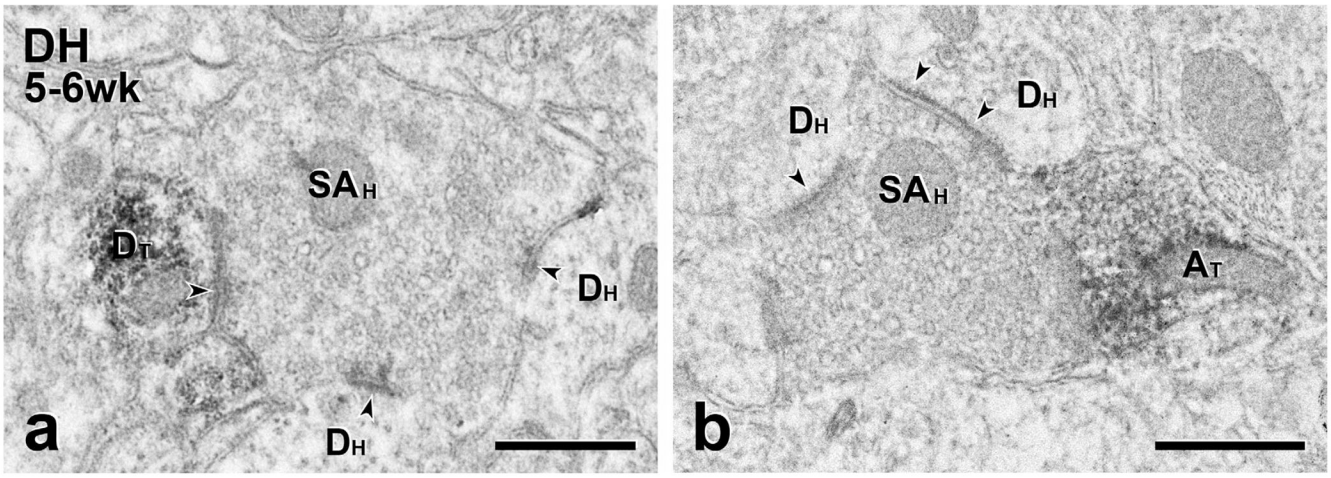

FIGURE 8.

Short-term transplants: MGE-derived neurons participate in synaptic glomeruli. (a) This unlabeled scalloped central terminal (SA_H), likely of primary afferent origin, is presynaptic to a GFP-positive transplant-derived dendrite (D_T) as well as to two unlabeled host dendrites (D_h). (b) This unlabeled scalloped terminal is also presynaptic to two unlabeled host dendrites (D_H) and directly contacts a GFP-positive transplant-derived axon terminal (A_T). Although a synaptic specialization is not apparent, there is no intervening glial process between the transplant-derived terminal and the scalloped terminal, suggesting that the MGE terminal is presynaptic to the host terminal. Scale bars: 500 nm

Author Manuscript Author Manuscript Author Manuscript Author Manuscript

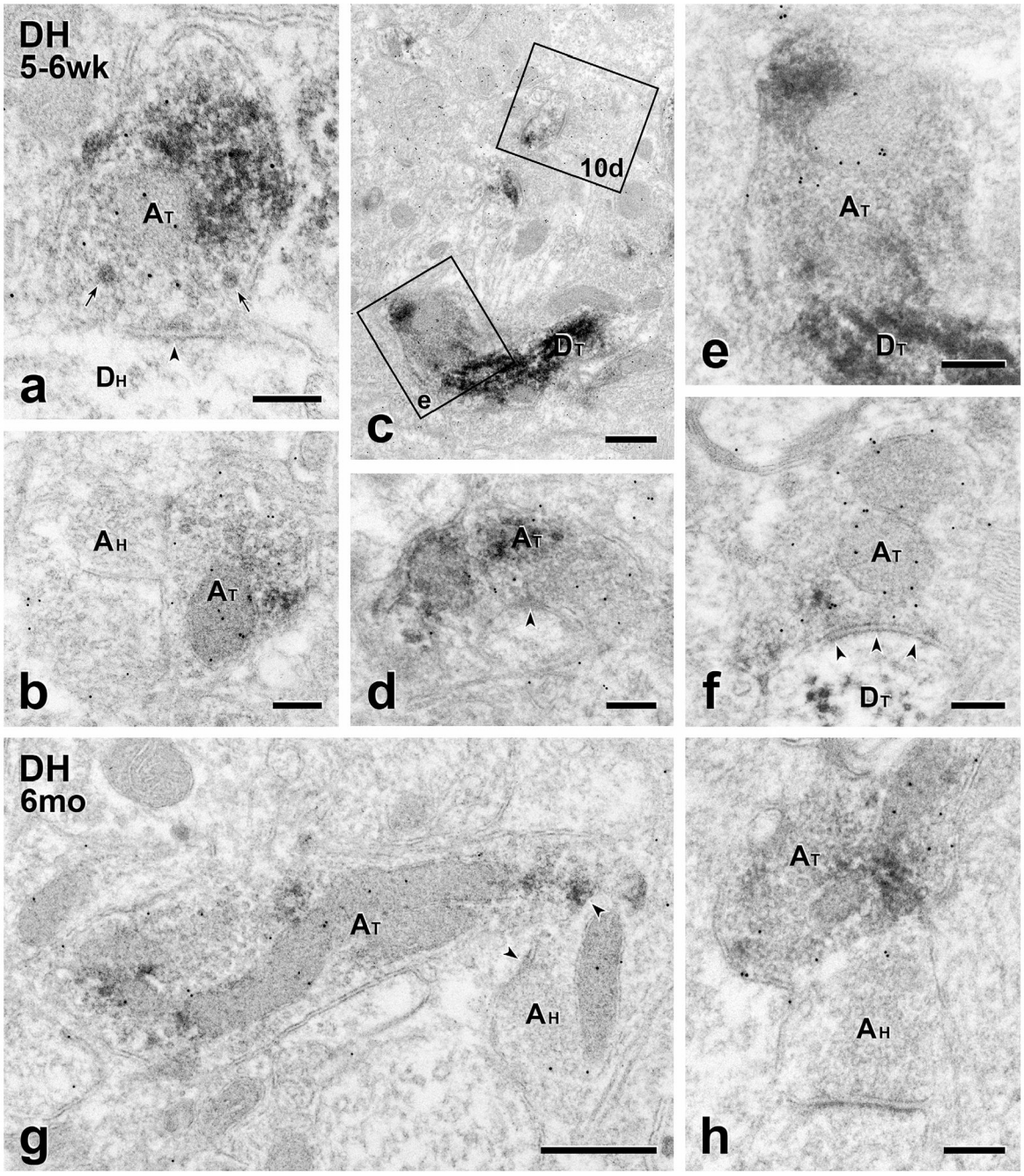

FIGURE 9.

Short- and long-term transplants: MGE-derived axon terminals are GABA-immunoreactive. (a–f) Short term transplants. GABA immunolabeling of GFP-immunoreactive MGE-derived axon terminals (A_T) with 10 nm gold illustrates the transmitter phenotype of transplant terminals and the breadth of the circuitry in which they engage. (a) A symmetric transplant-derived presynaptic input (arrowheads) to an unlabeled host dendrite (D_H). Both small clear and large granular vesicles (arrows) occur in the transplant terminal. (b) Axoaxonic apposition between transplant (GFP- and GABA-positive; A_T) and host-derived (GFP- and

Author Manuscript Author Manuscript Author Manuscript Author Manuscript

GABA-negative; A_H) terminals. (c) 10nm gold-immunolabeled transplant-derived dendrites (D_T). Boxed areas (e) and 10d are shown at higher magnification in Figures 9e and 10d, respectively. (d) Symmetric GABA-immunoreactive, transplant-derived (A_T) presynaptic input (arrowhead) to a small, unlabeled host dendrite. (e) A GABA-gold labeled transplant-derived terminal (A_T) directly contacts a transplant-derived dendrite (D_T). (f) Transplant-derived (A_T), GABA-immunoreactive symmetric input (arrowheads) to a transplant-derived dendrite (D_T). (g & h) Long term transplants. Transplant-derived, GABA-immunoreactive terminals (A_T) directly contact host axon terminals (A_H). The latter are presynaptic to unlabeled host dendrites. Scale bars: 500 nm in (c) and (g); 200 nm in all others

Author Manuscript Author Manuscript Author Manuscript Author Manuscript

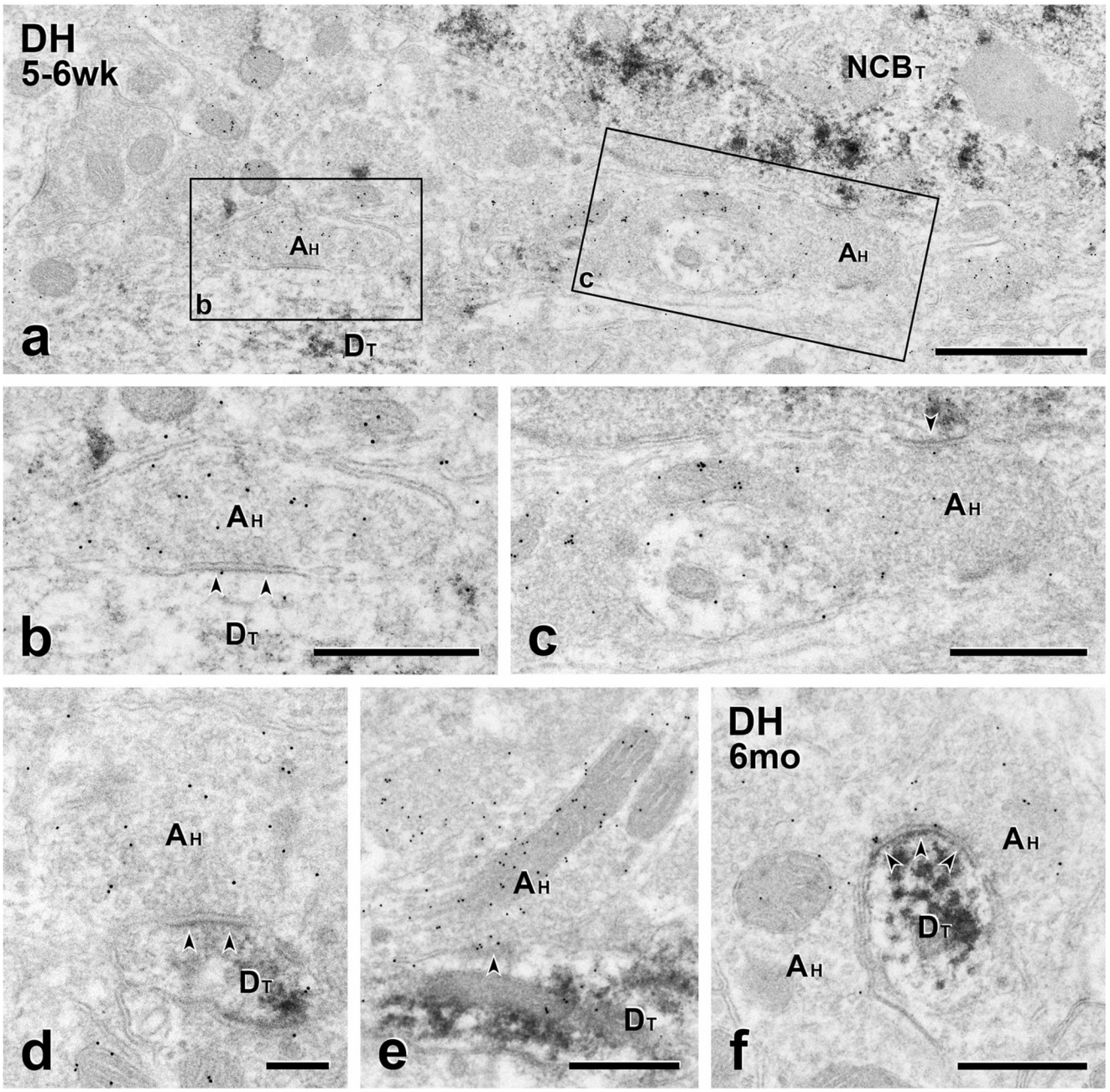

FIGURE 10.

Short- and long-term transplants: Host GABAergic neurons are presynaptic to transplant cell bodies and dendrites (a–e), Shortterm transplants. GFP-negative host axon terminals (A_H) labeled with 10 nm GABA immunogold form symmetric synapses on a GFP-positive, transplant-derived cell body (NCB_T in a) and dendrites (D_T in b, d and e). Boxed areas (b) and (c) are shown at higher magnification in panels (b) and (c), respectively. (f) Long-term transplant. 10 nm GABA immunogold labeled GFP-negative (host) axon terminal (A_H)

forms a symmetric synapse on a GFP-positive transplant-derived dendrite. Scale bars: 1 μm in (a); 500 nm in (b–f)

Author Manuscript Author Manuscript Author Manuscript Author Manuscript

Author Manuscript Author Manuscript Author Manuscript Author Manuscript

TABLE 1:

Primary antibodies used

Antigen	Immunogen	Manufacturer, Catalog number, RRID, Species antibody was raised in, Mono- vs. poly-clonal,	Dilution used
Green Fluorescent Protein (GFP)	Recombinant full length protein corresponding to GFP.	Abcam (Cambridge MA, USA), Catalog # ab13970, RRID: AB_300798,chicken polyclonal	1:10,000 and 1:20,000
γ-Aminobutyric Acid (GABA)	GABA conjugated to bovine serum albumin	Sigma (St Louis MO, USA), Catalog # A2052, RRID: AB_477652rabbit polyclonal	1:1,000

J Comp Neurol. Author manuscript; available in PMC 2018 November 29.

Author Manuscript

Author Manuscript

Author Manuscript

Author Manuscript

TABLE 2

Host input to MGE-derived, GFP-immunoreactive dendrites

	Dendrites			
Mouse	**Total**	**No input**	**Input**	**% with input**
Short-term transplants (5–6 weeks)				
1	139	67	72	51.8
2	80	32	48	60.0
3	167	79	88	52.7
4	110	47	63	57.3
5	103	55	49	47.6
Long-term transplants (5–6 months)				
6	99	22	77	77.7
7	72	13	59	81.9